

SIMULATED LUNAR ENVIRONMENT SPECTRA OF FELSIC ROCK PARTICULATES. T. D. Glotch¹, K. A. Shirley¹, and B. T. Greenhagen², ¹Department of Geosciences, Stony Brook University, Stony Brook, NY 11794-2100 (timothy.glotch@stonybrook.edu), ²Applied Physics Laboratory, Laurel, MD.

Introduction: Basaltic volcanics dominate the lunar secondary crust. However, since the Apollo era, anomalous regions characterized by mostly featureless red slopes in their visible/near-infrared (VNIR) spectra have been recognized. These “red spots” were suggested to result from non-basaltic volcanic activity. These early suggestions of non-mare volcanism were based on interpretations of rugged geomorphology resulting from viscous lava flows and relatively featureless, red-sloped VNIR spectra [1-4].

Mid-infrared (MIR) data from the Diviner instrument on the Lunar Reconnaissance Orbiter have confirmed that many of the red spot features are silicic volcanic domes. Additional detections of silicic material in the Aristarchus central peak and ejecta suggest excavation of a subsurface silicic pluton. [5-8]. All of these features are correlated with Th anomalies, further supporting the argument that they are the products of evolved magmas.

Identification of highly silicic materials on the Moon is based on the shape of three-point spectra using Diviner’s “8 micron channels” centered at 7.81, 8.28, and 8.55 μm (Figure 1). Typical lunar materials exhibit a concave-down spectral shape. In these cases, the spectra can be modeled as a parabola, and the maximum is taken as the Christiansen Feature (CF) position, which is indicative of the degree of silica polymerization. Felsic materials typically have CF positions at shorter wavelengths, while more mafic materials have CF positions at longer wavelengths. In contrast, highly silicic regions have concave up Diviner spectra because their CF positions are at shorter wavelengths, and Diviner’s 8 micron channels fall within the silicate Reststrahlen bands. For these materials, the CF position cannot be determined. However, the concavity of the Diviner spectra can be mapped (Figure 2), providing an easy way to identify silicic features on the lunar surface [5-6].

To date, the SiO_2 content of the silicic dome features has been difficult to quantitatively determine due to the limited spectral resolution of Diviner and lack of terrestrial analog spectra acquired in an appropriate environment. Based on spectra of pure mineral and glass separates, preliminary estimates suggest that the rocks comprising the lunar silicic domes are > 65 wt.% SiO_2 . In an effort to better constrain this value, we have acquired spectra of andesite, rhyolite, pumice, and obsidian rock samples under a simulated lunar environment (SLE) in the Planetary and Asteroid Regolith

Spectroscopy Environmental Chamber (PARSEC) at the Center for Planetary Exploration at Stony Brook

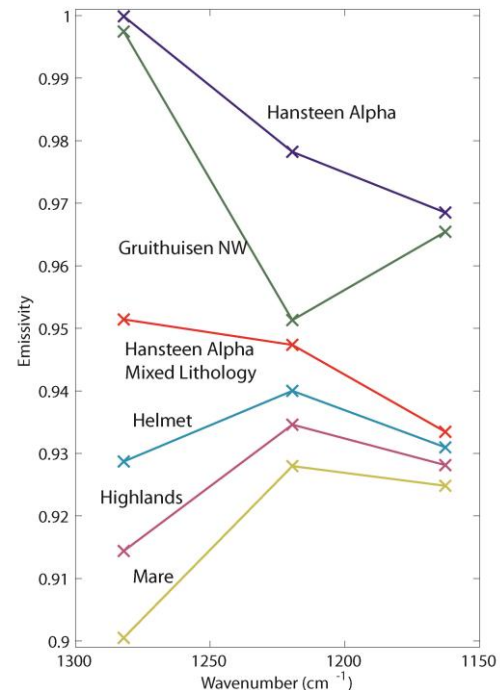


Figure 1. Diviner 3-point spectra of silicic regions (Hansteen Alpha and the Gruithuisen NW dome), and more typical lunar surfaces, including a non-silicic red spot (Helmet). Figure adapted from [x].

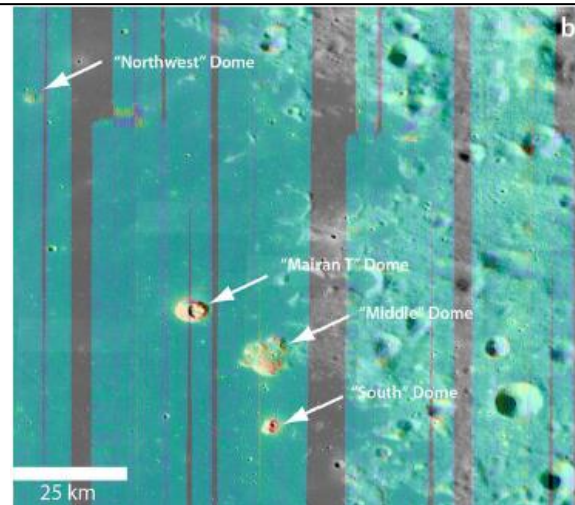


Figure 2. Diviner concavity index map in the Mairan domes region, highlighting the unique silicic composition of the Mairan domes. Figure adapted from [6].

University. In this work, we present spectra of these materials and discuss how they relate to the Diviner measurements of the lunar silicic dome features.

Methods: Hand samples of andesite, rhyolite, pumice, and obsidian were acquired from Wards Natural Science, ground, and dry sieved to seven size fractions: <32 μm , 32-63 μm , 63-90 μm , 90-125 μm , 125-180 μm , 180-250 μm , and > 250 μm . MIR emission spectra were acquired under ambient and simulated lunar environment conditions in the PARSEC chamber at Stony Brook University. PARSEC simulates the lunar environment by pumping to a pressure of $<10^{-5}$ mbar, cooling a radiation shield to $< -120^{\circ}\text{C}$, and heating samples from both above and below, according to the methods of [9-10].

Results: Full resolution SLE spectra of rhyolite are shown in Figure 3, and those same spectra convolved to the Diviner bandpasses are shown in Figure 4. Comparable spectra were also acquired for andesite, obsidian, and rhyolite. As can be seen in Figure 3, the CF position shifts to shorter wavelengths with decreasing size fraction. In addition, the spectral contrast increases

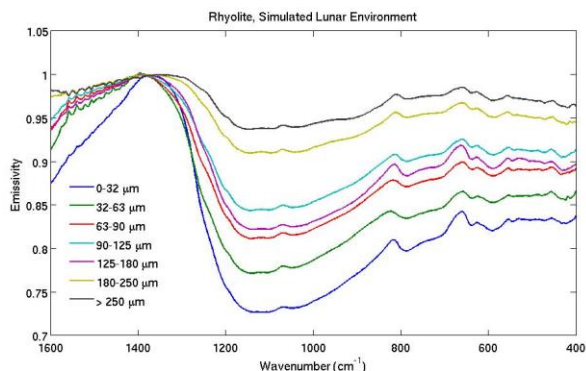


Figure 3. Simulated lunar environment spectra of seven rhyolite size fractions.

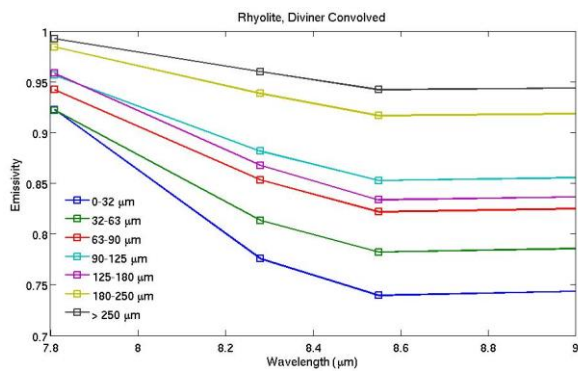


Figure 4. Diviner-resolution SLE spectra of seven rhyolite size fractions.

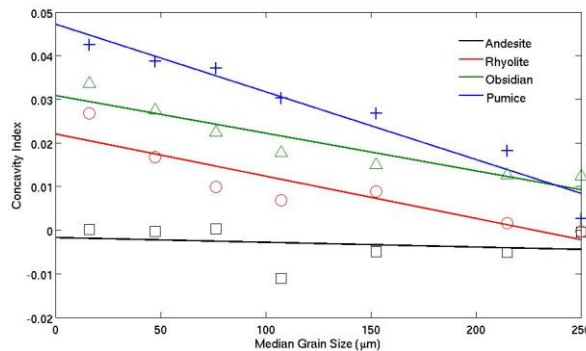


Figure 5. Concavity index (defined by [x]) vs. size fraction for andesite, rhyolite, obsidian, and pumice.

es as the size fraction decreases. This trend is opposite to what is seen for spectra collected in ambient environments, but has also been documented for pure mineral separates under SLE conditions [11]. When convolved to the Diviner bandpasses, it is clear that the spectral shape measured by Diviner is sensitive to grain size as well as composition.

Figure 5 shows the relationship between the Diviner concavity index [5] and grain size for the four compositions measured here. With the exception of andesite, which has index values near zero for every size fraction, all size fractions of all samples have positive concavity index values, with index values increasing as grain size decreases.

Discussion and Conclusions: Each of the rhyolite, obsidian, and pumice samples have spectral characteristics consistent with the Diviner spectra of silicic regions. In general, andesite spectra, when convolved to Diviner spectral sampling have low concavity index values, which are inconsistent with Diviner’s measurements of silicic regions. The spectral shapes of the silicic rock particulates measured for this work are strongly dependent on particle size (Figure 5). This suggests that, in addition to composition and space weathering, Diviner’s measurements of thermal emission in the CF region are also sensitive to particle size.

References: [1] Whitaker, E.A. (1972) *Moon*, **4**, 348. [2] Malin, M. (1974) *Earth Planet. Sci. Lett.*, **21**, 331. [3] Head J. W. & McCord T. B. (1978) *Science*, **199**, 1433. [4] Head et al. (1978) *9th LPSC, Abst.# 488*. [5] Glotch, T.D. et al. (2010) *Science*, **329**, 1510. [6] Glotch, T.D. et al. (2011) *GRL*, **38**, L21204. [7] Ashley, J.W. (2016) *Icarus*, **273**, 248. [8] Jolliff, B.L. et al. (2011) *Nature Geosci.*, **4**, 566. [9] Thomas, I. R. et al. (2012), *Rev. Sci. Inst.*, **83**, 124502. [10] Donaldson Hanna et al. (2012), *JGR Planets*, **117** (E12). [11] Shirley, K. A., and T. D. Glotch (2016), *Lunar Planet. Sci. XLVII*, abstract 2552.